

Body-centered superhard BC₂N phases from first principles

Xiaoguang Luo, Xiaoju Guo, Bo Xu, Qinghua Wu, Qianku Hu, Zhongyuan Liu, Julong He, Dongli Yu, and Yongjun Tian*
State Key Laboratory of Metastable Materials Science and Technology, Yanshan University, Qinhuangdao 066004, China

Hui-Tian Wang

National Laboratory of Solid State Microstructures and Department of Physics, Nanjing University, Nanjing 210093, China

(Received 18 April 2007; revised manuscript received 9 August 2007; published 7 September 2007)

Body-centered BC₂N deduced from the unit cell of the recently predicted body-centered carbon [F. J. Ribeiro *et al.*, Phys. Rev. B **74**, 172101 (2006)] are studied with first-principles pseudopotential density functional method. The structural, electronic, and mechanical properties are investigated for 11 possible atomic configurations of body-centered BC₂N. Our results show that the *sp*³-bonded body-centered BC₂N phases have lower density than the previously investigated *sp*³-bonded zinc-blende BC₂N, wurtzite BC₂N, and chalcopyrite BC₂N. The struc-A and struc-B composed of the maximum numbers of C-C and B-N bonds have the lowest total energy among the investigated body-centered BC₂N structures. Their calculated bulk moduli are 305 and 309 GPa, respectively. The theoretical Vickers hardness of the body-centered BC₂N is over 60 GPa, indicating that it is a potential superhard material with the hardness comparable to cubic boron nitride.

DOI: 10.1103/PhysRevB.76.094103

PACS number(s): 61.50.Ah, 81.05.Zx, 71.15.Mb, 62.20.Qp

I. INTRODUCTION

The search for new superhard materials is an important research field in modern science and technology. In this field, boron-carbonitride (B-C-N) compounds attract more attention since the prediction of superhard β-C₃N₄ compound.¹ Experimentally, various synthesis methods have been used to synthesize hexagonal, cubic, and amorphous B-C-N materials, such as chemical vapor deposition,² solvothermal method,³ chemical process method,⁴ high temperature and high pressure (HTHP) method,^{5–8} mechanical alloyed method,⁹ spark plasma sintering,¹⁰ shock-wave compression method,¹¹ etc. So far, nanocrystalline BC₂N with cubic structure⁷ (*c*-BC₂N) has been synthesized from graphitelike BC₂N (Ref. 4) by the HTHP method using diamond anvil cell and large volume press. The experimentally measured Vickers hardness of *c*-BC₂N is 76 GPa,⁷ which is harder than 66 GPa of cubic boron nitride (*c*-BN). On the one hand, the measured bulk modulus of 259±22 GPa (or 282 GPa) from Brillouin scattering¹² (or from x-ray diffraction⁷) is not in agreement with the calculated high bulk modulus (355–402 GPa) of the predicted zinc-blende BC₂N (ZB-BC₂N), whose high bulk modulus should result in high Vickers hardness.^{13,14} On the other hand, the accurate atomic positions in the *c*-BC₂N crystal could not be determined conclusively by using Rietveld refinement because the atomic numbers of B, C, and N are quite adjacent. Thus, how many polymorphs BC₂N has is still an open question at present. Therefore, it is important to explore possible crystal structures using first-principles methods for a deep understanding of BC₂N polymorphs.

Since isoelectronic BC₂N compound is the ideal mixing of carbon and boron nitride (BN) as viewed from composition, it is reasonable to speculate that the BC₂N compound should have the similar crystal structures to carbon and BN. Most of the previous experimental and theoretical studies on this topic originated from this clue. For the *sp*³-bonded BC₂N phases, the theoretically studied structures are all high

dense phases, such as ZB-BC₂N,^{13,14} wurtzite BC₂N (WZ-BC₂N),^{15,16} and chalcopyrite BC₂N.¹⁷ Recently, a hypothetical body-centered *sp*³-bonded carbon (named bc6-C thereafter) with lower density than diamond was proposed in order to explore the structure of Popigai carbon obtain from an impact crater.¹⁸ Generally, under extreme conditions, such as at earth center, the transition-state phases can be reserved more easily for multicomponent compounds than for pure elements due to dynamic factors. Therefore, we investigate the lower-density *sp*³-bonded BC₂N (bc6-BC₂N) starting from the hypothetical bc6-C structure. The updated semi-empirical formula of hardness for polar covalent solids makes the hardness estimation of bc6-BC₂N possible.^{19,20} In this paper, we report the possible configurations and Vickers hardness of bc6-BC₂N deduced from the hypothetical bc6-C carbon.

II. CALCULATION

The first-principles calculations are performed using the pseudopotential density functional method with the CASTEP code.²¹ Exchange and correlation effects are described by the CA-PZ in the local density approximation.^{22,23} The norm-

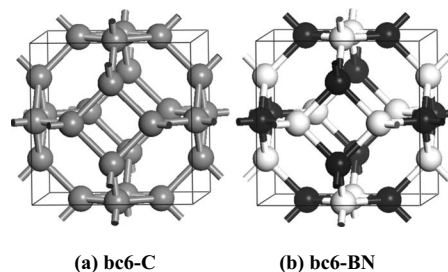


FIG. 1. Unit cells of hypothetical (a) bc6-C and (b) bc6-BN. The carbon, boron, and nitrogen are depicted in gray, white, and black colors, respectively.

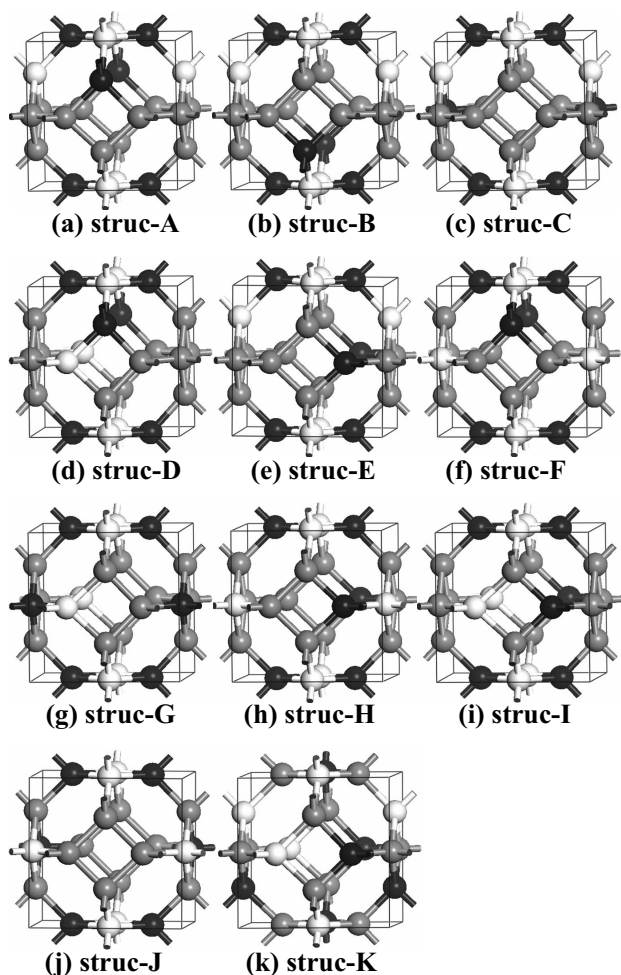


FIG. 2. Considered 11 configurations of bc6-BC₂N (after structural relaxation) starting from the hypothetical bc6-C unit cell.

conserving pseudopotential is expanded within a plane wave basis set with an energy cutoff of 770 eV.²⁴ The integrations in the Brillouin zone are performed according to the Monkhorst-Pack scheme with the k points of $6 \times 6 \times 6$ grid.²⁵ All the structures are relaxed by the BFGS methods.²⁶ The Mulliken overlap populations were integrated by a distance cutoff 3 Å.

III. STRUCTURAL CONSTRUCTION

The hypothetical bc6-C shown in Fig. 1(a) has the body-centered cubic structure with the symmetry of $Im\bar{3}m$ (space group No. 229).¹⁸ There are 12 atoms in its unit cell and all the atoms are fourfold coordinated with the other atoms. Starting from this unit cell, only one configuration for BN (named bc6-BN) can be constructed, as shown in Fig. 1(b), if no B-B and N-N bond forms. However, the large number of nonequivalent atomic configurations of bc6-BC₂N structures can be constructed by replacing the six carbon atoms in the unit cell with three boron atoms and three nitride atoms. In the present study, we mainly focused on the bc6-BC₂N structures with relative lower total energy, which should be relatively stable.

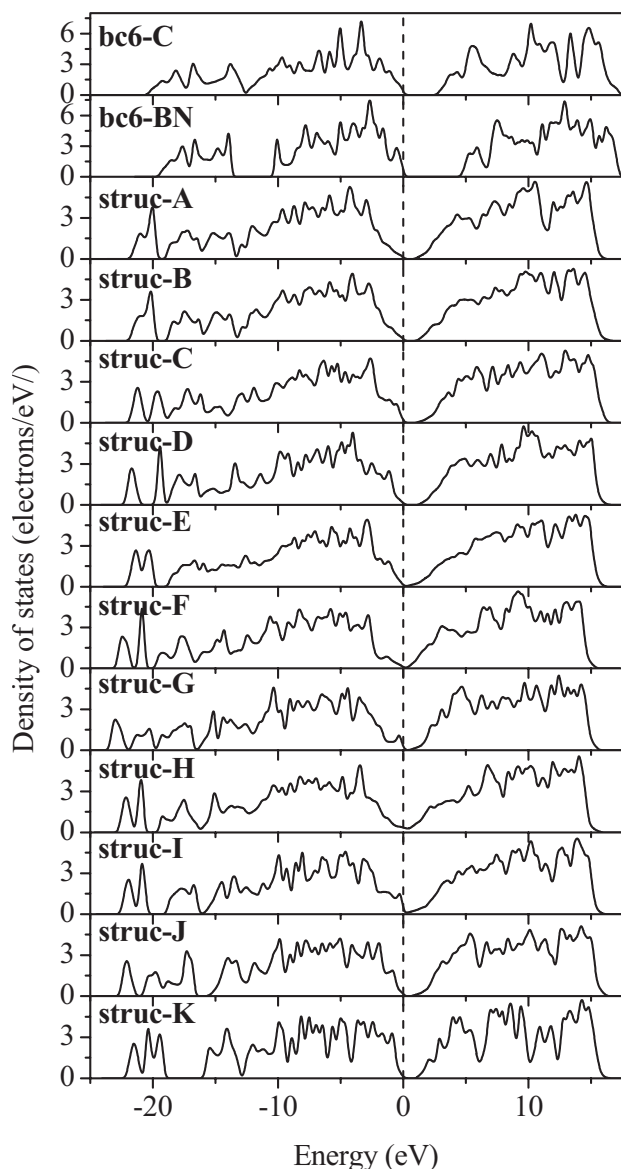


FIG. 3. Calculated total density states of bc6-C, bc6-BN, and the 11 hypothetical configurations of bc6-BC₂N.

The previous theoretical studies have shown that the B-B bond and N-N bond should not exist in the structures of B-C-N compounds.^{13,27} This result is quite different from the fact that single-bonded N-N bond exists in the structures of recently synthesized superhard heavy metal compounds such as PtN₂ and IrN₂.^{28,29} According to the bond-counting rule, the BC₂N structures with the maximum numbers of C-C and B-N bonds should have the lowest total energy. In other words, B-C and C-N bonds should be unfavorable.^{15,30} In order to construct the structures of bc6-BC₂N from bc6-C, we have to substitute six carbon atoms with three boron atoms and three nitrogen atoms. Because four atoms locate on each face of the bc6-C unit cell, as shown in Fig. 1(a), it is ideal for one face to be composed of two B atoms and two N atoms or for each face composed of one BC₂N formula. Now, let us construct the possible configurations composed of two B atoms and two N atoms on one face of bc6-BC₂N

TABLE I. Equilibrium lattice parameters, densities (ρ), total energy (E_t), total energy difference (ΔE), bulk modulus (B), and type and number of chemical bond for hypothetical bc6-C, bc6-BN, and bc6-BC₂N.

Structure	bc6-C	bc6-BN	Struc-A	Struc-B	Struc-C	Struc-D	Struc-E	Struc-F	Struc-G	Struc-H	Struc-I	Struc-J	Struc-K
Symmetry	<i>Im-3m</i>	<i>Pm-3n</i>	<i>Pmm2</i>	<i>Pmm2</i>	<i>Pm</i>	<i>Pm</i>	<i>Pm</i>	<i>Pm</i>	<i>Pm</i>	<i>Pm</i>	<i>Pmm2</i>	<i>Pmm2</i>	<i>R32</i>
a (Å)	4.326	4.402	4.361	4.362	4.359	4.374	4.357	4.355	4.386	4.334	4.360	4.406	4.434
b (Å)	4.326	4.402	4.382	4.387	4.359	4.373	4.414	4.400	4.399	4.433	4.443	4.416	4.434
c (Å)	4.326	4.402	4.405	4.401	4.403	4.402	4.405	4.422	4.377	4.420	4.379	4.404	4.434
α (deg)	90.00	90.00	90.00	90.00	90.00	89.93	89.88	90.00	90.00	90.00	90.00	90.00	89.65
β (deg)	90.00	90.00	90.00	90.00	89.97	90.00	90.00	89.92	90.00	90.00	90.00	90.00	90.35
γ (deg)	90.00	90.00	90.00	90.00	90.00	90.00	90.00	90.00	90.06	89.99	90.00	90.00	89.65
Volume (Å ³)	80.97	85.28	84.19	84.22	84.38	84.20	84.71	84.73	84.45	84.91	84.85	85.69	87.17
ρ (g/cm ³)	2.956	2.900	2.890	2.889	2.883	2.890	2.872	2.871	2.881	2.865	2.867	2.839	2.791
E_t (eV/atom)	-155.01	-175.38	-164.92	-164.91	-164.85	-164.84	-164.77	-164.76	-164.69	-164.69	-164.61	-164.61	-164.27
ΔE (eV/atom)			0.666	0.671	0.732	0.745	0.810	0.827	0.892	0.888	0.976	0.971	1.310
B (GPa)	344	298	305	309	303	305	301	296	297	292	295	282	270
No. C-C bond	24	0	8	8	7	7	6	6	5	5	4	4	0
No. B-N bond	0	24	8	8	7	7	6	6	5	5	4	4	0
No. B-C bond	0	0	4	4	5	5	6	6	7	7	8	8	12
No. C-N bond	0	0	4	4	5	5	6	6	7	7	8	8	12

structures, which yields to the bond-counting rule. This procedure involves in two steps. Firstly, we make two -B-N-B-N-B- rings locate on two opposite (001) faces of the bc6-BC₂N unit cell, which means that two boron atoms and two nitrogen atoms are settled down. Secondly, we will consider the locations of one left boron atom and one left nitrogen atom in the unit cell. Thus, we obtain only ten non-equivalent atomic configurations of the bc6-BC₂N structures. These ten configurations are demonstrated in Figs. 2(a)–2(j) in order of the numbers of B-N (C-C) bonds. As shown in Fig. 2(k), we also give a special example of the configurations where each face is composed of one BC₂N formula for comparison. Obviously, there are no favorable C-C and B-N bonds in this special structure.

IV. RESULTS AND DISCUSSION

The structural parameters, the total energy E_t , and the types and numbers of chemical bond of bc6-C and bc6-BN in Figs. 1(a) and 1(b), and bc6-BC₂N with the constructed atomic configurations in Figs. 2(a)–2(k) are listed in Table I. After relaxation, the considered bc6-BC₂N structures exhibit three kinds of symmetries of *Pm*, *Pmm2*, and *R32*, different from *Im-3m* symmetry of the bc6-C structure. The equilibrium lattice constants (a , b , and c) of all the presented bc6-BC₂N structures are larger than those of the bc6-C structure. It should be noted that one of the interaxial angles (α , β , and γ) in the suggested bc6-BC₂N structures with *R32* and *Pm* symmetries departs from 90° slightly, while they are not changed in the structures with *Pmm2* symmetry. As shown in Table I, struc-A and struc-B have the lowest total energies among the 11 bc6-BC₂N structures because they have the maximum numbers of the C-C bond and the B-N bond in the unit cell. It is found that struc-A with the lowest total energy has a sandwich structure and struc-B with the

second lowest total energy has a sandwichlike structure. This indicates that BC₂N prefers to form the sandwich structures rather than nonsandwich structures, which is in accordance with the previously investigated sandwich ZB-BC₂N,¹³ sandwich WZ-BC₂N,¹⁶ or even the sandwich sp^2 -bonded BC₂N.³¹

In order to investigate the stability of different configurations for bc6-BC₂N, the total energy difference of $\Delta E = E_{\text{bc6-BC}_2\text{N}} - (E_{\text{diamond}} + E_{c\text{-BN}})/2$ is used here. As shown in Table I, ΔE has positive value for the configurations of bc6-BC₂N, indicating that they are metastable phases and tend to separate into diamond and *c*-BN. Struc-A of bc6 structure has larger ΔE than struc-1 and struc-2 of ZB structures,¹³ which means that struc-1 and struc-2 are relatively stable than struc-A. The tendency of phase separation for bc6-BC₂N is quite similar to those for the sp^3 -bonded ZB-BC₂N,^{13,14} wurtzite BC₂N,^{15,16} and chalcopyrite BC₂N,¹⁷ implying that the phase separation is one common problem for experimentally synthesizing sp^3 -bonded BC₂N. In order to further check the mechanical stability of these bc6-BC₂N structures, their elastic stiffness constants are calculated by using the finite strain techniques in the CASTEP package. Because the criteria of the mechanical stability for the structures with three kinds of symmetries mentioned above are different, here we give only an example for the orthorhombic struc-A with the lowest total energy. For an orthorhombic crystal, there are nine independent elastic stiffness constants ($c_{11}, c_{22}, c_{33}, c_{44}, c_{55}, c_{66}, c_{12}, c_{13}, c_{23}$), and the mechanical restrictions of the elastic stiffness constants are³²

$$(c_{11} + c_{22} - 2c_{12}) > 0,$$

$$(c_{11} + c_{33} - 2c_{13}) > 0,$$

$$(c_{22} + c_{33} - 2c_{23}) > 0,$$

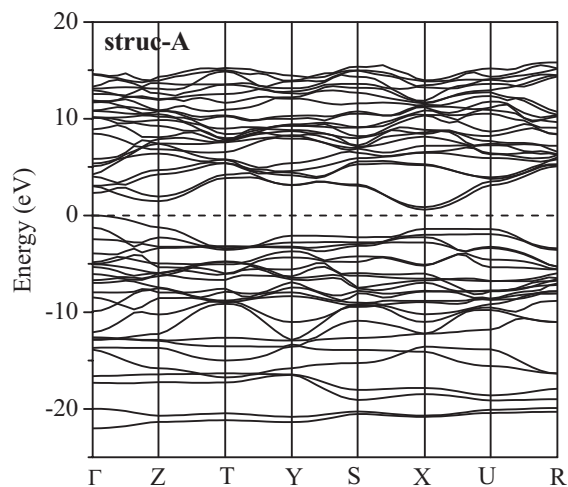


FIG. 4. Calculated band structure of struc-A.

$$c_{11} > 0, \quad c_{22} > 0, \quad c_{33} > 0, \quad c_{44} > 0, \\ c_{55} > 0, \quad c_{66} > 0,$$

$$(c_{11} + c_{22} + c_{33} + 2c_{12} + 2c_{13} + 2c_{23}) > 0.$$

The calculated elastic stiffness constants of struc-A are $c_{11}=643$ GPa, $c_{22}=835$ GPa, $c_{33}=734$ GPa, $c_{44}=260$ GPa, $c_{55}=220$ GPa, $c_{66}=251$ GPa, $c_{12}=97$ GPa, $c_{13}=105$ GPa, and $c_{23}=75$ GPa. Obviously, the calculated elastic stiffness constants satisfy all of the above mechanical stability conditions, indicating that struc-A is stable mechanically.

In Fig. 3, we plot the electronic density of states of the 11 hypothetical bc6-BC₂N structures, as well as those of the bc6-C and the bc6-BN. From the total density of states, it seems that struc-E, struc-F, struc-H, and struc-I should be metallic, while the other structures should be semiconductive. The calculated energy gaps of struc-A, struc-B, struc-C, struc-D, struc-G, struc-J, and struc-K are 0.60 eV, 0.72 eV, 0.83 eV, 0.93 eV, 0.26 eV, 0.40 eV, and 0.79 eV, respectively. Obviously, the energy gaps of these seven structures are much less than the gap (2.52 eV) of the hypothetical bc6-C or the gap (4.42 eV) of the hypothetical bc6-BN. For zinc-blende and wurtzite structures, similar results were also reported,^{13,16} i.e., the energy gaps of the ZB-BC₂N or WZ-BC₂N phases are smaller than that of diamond or lonsdaleite. The calculated band structure of struc-A is shown in Fig. 4. Struc-A with band gap of 0.60 eV is an indirect semiconductor such as bc6-C, bc6-BN, diamond, and *c*-BN. The top of its valence band is at the Γ point, while the bottom of its conduction band is at the X point.

As shown in Table I, struc-A and struc-B have the largest density (2.890 g/cm³) among the 11 bc6-BC₂N structures, being lower than not only those of bc6-C (2.956 g/cm³) and bc6-BN (2.900 g/cm³) but also *sp*³-bonded ZB-BC₂N,¹³ WZ-BC₂N,¹⁶ chalcopyrite BC₂N,¹⁷ and experimentally synthesized *c*-BC₂N.⁷ Because the bulk modulus of a crystal is dependent roughly on its density, struc-A and struc-B exhibit high bulk moduli of 305 and 309 GPa, respectively. From the data of bulk moduli for struc-A and struc-B, they should

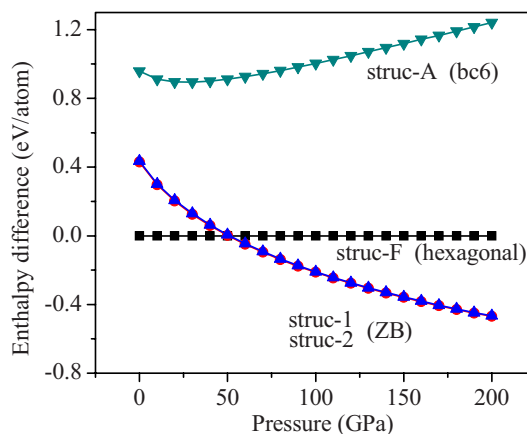


FIG. 5. (Color online) Calculated enthalpy differences as a function of pressure for the relatively stable struc-A among bc6 BC₂N structures, struc-F among hexagonal BC₂N structures from Ref. 31, and struc-1 (struc-2) among ZB BC₂N structures from Ref. 13. The enthalpy of hexagonal struc-F is selected as the reference.

belong to superhard materials. We also estimate their Vickers hardness. As shown in Table II, there are three types of C-C bonds, three types of B-N bonds, two types of C-N bonds, and two types of B-C bonds in struc-A and struc-B, which indicates that struc-A and struc-B belong to complex crystals. From the point of view of chemical bonding, the chemical bonds in the two structures are composed of main covalent component and partial ionic component, and no metallic component. Therefore, our microscopic model of hardness^{19,20} is valid for the hardness estimation of struc-A and struc-B. Their Vickers hardness can be calculated as follows:

$$H_V = [H_V^{C1-C1} H_V^{C1-N1} (H_V^{C2-C2})^2 H_V^{C3-C3} H_V^{B1-N1} H_V^{C2-N2} \\ \times (H_V^{B2-N2})^2 H_V^{B1-C1} H_V^{B2-C2} H_V^{B3-N3}]^{1/12},$$

where $H_V^{X-Y} = 350(N_e^{X-Y})^{2/3} e^{-1.191 f_i^{X-Y} / (d^{X-Y})^{2.5}}$ is the hardness of hypothetical binary compound composed of X-Y bond. N_e^{X-Y} is the valence electron densities of the hypothetical compounds composed of X-Y bond. According to our generalized ionicity scale,²⁰ the Phillips ionicity f_i^{X-Y} of X-Y bond can be calculated as $f_i^{X-Y} = (f_h^{X-Y})^{0.735} = [1 - \exp(-|P_c - P^{X-Y}| / P^{X-Y})]^{0.735}$, where f_h^{X-Y} is the ionicity scale of the X-Y bond based on bond overlap population, P^{X-Y} is the overlap population of the X-Y bond, and P_c is the overlap population of the bond in a pure covalent crystal containing the same type of chemical bond. Here, we select a pure covalent crystal of bc6-C to determine P_c . Because the calculated overlap population of every C-C bond in the bc6-C structure is 0.78, we use $P_c=0.78$ for the chemical bonds in the bc6-BC₂N structures. The bond number n_i , bond length d^{X-Y} , bond population P^{X-Y} , valence electron densities N_e^{X-Y} , ionicities f_h^{X-Y} and f_i^{X-Y} , and H_V^{X-Y} for each type of chemical bond for struc-A and struc-B are listed in Table II. Based on the calculated data, struc-A and struc-B have comparable Vickers hardness with *c*-BN, indicating that they are potential superhard materials. Because of the lower density and

TABLE II. Bond parameters and the calculated Vickers hardness of hypothetical struc-A and struc-B.

	Bond type	n_l	d^{X-Y} (Å)	ρ^{X-Y}	N_e^{X-Y}	f_h^{X-Y}	f_i^{X-Y}	H_V^{X-Y}	H_V (GPa)
Struc-A	C1–C5	2	1.495	0.8	0.635	0.025	0.066	87.4	65
	C4–N1	2	1.512	0.66	0.553	0.166	0.267	61.0	
	C2–C5	4	1.529	0.79	0.595	0.013	0.040	81.7	
	C2–C4	2	1.550	0.83	0.571	0.058	0.124	69.4	
	B3–N1	2	1.551	0.60	0.608	0.259	0.371	53.9	
	C5–N3	2	1.551	0.61	0.512	0.243	0.354	49.1	
	B1–N2	4	1.552	0.64	0.606	0.196	0.302	58.2	
	B1–C1	2	1.562	0.80	0.651	0.025	0.066	79.8	
	B3–C3	2	1.602	0.76	0.602	0.026	0.068	70.8	
B1–N3	2	1.612	0.65	0.541	0.181	0.285	50.1		
Struc-B	C1–C5	2	1.524	0.81	0.600	0.036	0.088	78.2	64
	C4–N1	2	1.495	0.66	0.573	0.166	0.267	64.3	
	C2–C5	4	1.535	0.79	0.588	0.013	0.040	80.3	
	C2–C4	2	1.535	0.82	0.588	0.048	0.107	74.2	
	B3–N1	2	1.568	0.6	0.588	0.259	0.371	51.3	
	C5–N3	2	1.514	0.61	0.551	0.243	0.354	54.7	
	B1–N2	4	1.558	0.64	0.600	0.196	0.302	57.3	
	B1–C1	2	1.600	0.85	0.606	0.079	0.155	64.3	
	B3–C3	2	1.616	0.79	0.588	0.013	0.040	70.5	
B1–N3	2	1.566	0.62	0.591	0.227	0.337	53.7		

bulk modulus, the theoretical Vickers hardness of struc-A and struc-B is smaller than those of sp^3 -bonded ZB-BC₂N,¹⁴ WZ-BC₂N,¹⁶ and chalcopyrite BC₂N.¹⁷

At last, we calculated the enthalpy as a function of pressure for struc-A, struc-F among the hexagonal BC₂N structures from Ref. 31, and struc-1 and struc-2 among ZB BC₂N structures from Ref. 13. The enthalpy differences of bc6 and ZB BC₂N structures relative to hexagonal BC₂N structure are shown in Fig. 5. In the hydrostatic pressure range of 0–200 GPa, our first-principles calculation results show that struc-A cannot be directly synthesized from the hexagonal or ZB BC₂N phases due to the existence of the larger energy barrier. This result is quite similar to the reported results of bc6-C, in which the bc6-C phase could not be obtained directly from graphite or diamond under the hydrostatic pressure.¹⁸ Under extreme nonequilibrium conditions such as the condition of ultrahigh pressure and ultrahigh temperature obtained in very short time, however, the formation of metastable bc6-BC₂N phase becomes possible because the long-distance diffusions of B, C, and N atoms required for the formation of stable BC₂N phase are impossible.

V. CONCLUSIONS

Using first-principles pseudopotential density functional method, we have investigated the structural, electronic, and mechanical properties of the 11 possible atomic arrangements for the bc6-BC₂N deduced from the recently predicted body-centered carbon. Our calculation results show that the bc6-BC₂N phases are the low density phases in the investigated sp^3 -bonded BC₂N. Struc-A and struc-B with the maximum numbers of C-C bond and B-N bond have the lowest total energy in the considered 11 bc6-BC₂N structures. Their bulk moduli are 305 and 309 GPa, respectively, close to the experimental value of the synthesized *c*-BC₂N. The theoretical Vickers hardness over 60 GPa indicates that bc6-BC₂N is one potential superhard material comparable to *c*-BN.

ACKNOWLEDGMENTS

This work was supported by PCSIRT, NSFC (Grant Nos. 10325417, 50472051, and 50532020) and NBRPC (Grant No. 2005CB724400).

*Corresponding author. fhcl@ysu.edu.cn

- ¹A. Y. Liu and M. L. Cohen, *Science* **245**, 841 (1989).
- ²R. B. Kaner, J. Kouvetakis, C. E. Warble, M. L. Sattler, and N. Bartlett, *Mater. Res. Bull.* **22**, 399 (1987).
- ³F. L. Huang, C. B. Cao, X. Xiang, R. T. Lv, and H. S. Zhu, *Diamond Relat. Mater.* **13**, 1757 (2004).
- ⁴M. Hubacek and T. Sato, *J. Solid State Chem.* **114**, 258 (1995).
- ⁵S. Nakano, M. Akaishi, T. Sasaki, and S. Yamaoka, *Chem. Mater.* **6**, 2246 (1994).
- ⁶E. Knittle, R. B. Kaner, R. Jeanloz, and M. L. Cohen, *Phys. Rev. B* **51**, 12149 (1995).
- ⁷V. L. Solozhenko, D. Andrault, G. Fiquet, M. Mezouar, and D. C. Rubie, *Appl. Phys. Lett.* **78**, 1385 (2001).
- ⁸Y. Zhao, D. W. He, L. L. Daemen, T. D. Shen, R. B. Schwarz, Y. Zhu, D. L. Bish, J. Huang, J. Zhang, G. Shen, J. Qian, and T. W. Zerda, *J. Mater. Res.* **17**, 3139 (2002).
- ⁹B. Yao, W. J. Chen, L. Liu, B. Z. Ding, and W. H. Su, *J. Appl. Phys.* **84**, 1412 (1998).
- ¹⁰X. G. Luo, J. X. Zhang, X. J. Guo, G. L. Zhang, J. L. He, D. L. Yu, Z. Y. Liu, and Y. J. Tian, *J. Mater. Sci.* **41**, 8352 (2006).
- ¹¹T. Komatsu, M. Nomura, Y. Kakudate, and S. Fujiwara, *J. Mater. Chem.* **6**, 1799 (1996).
- ¹²S. N. Tkachev, V. L. Solozhenko, P. V. Zinin, M. H. Manghnani, and L. C. Ming, *Phys. Rev. B* **68**, 052104 (2003).
- ¹³H. Sun, S. H. Jhi, D. Roundy, M. L. Cohen, and S. G. Louie, *Phys. Rev. B* **64**, 094108 (2001).
- ¹⁴X. J. Guo, Z. Y. Liu, X. G. Luo, D. L. Yu, J. L. He, and Y. J. Tian, *Diamond Relat. Mater.* **16**, 526 (2007).
- ¹⁵M. Mattesini and S. F. Matar, *Comput. Mater. Sci.* **20**, 107 (2001).
- ¹⁶X. G. Luo, X. J. Guo, Z. Y. Liu, J. L. He, D. L. Yu, B. Xu, H. T. Wang, and Y. J. Tian, *Phys. Rev. B* (to be published).
- ¹⁷J. Sun, X. F. Zhou, G. R. Qian, J. Chen, Y. X. Fan, H. T. Wang, X. J. Guo, J. L. He, Z. Y. Liu, and Y. J. Tian, *Appl. Phys. Lett.* **89**, 151911 (2006).
- ¹⁸F. J. Ribeiro, P. Tangney, S. G. Louie, and M. L. Cohen, *Phys. Rev. B* **74**, 172101 (2006).
- ¹⁹F. M. Gao, J. L. He, E. D. Wu, S. M. Liu, D. L. Yu, D. C. Li, S. Y. Zhang, and Y. J. Tian, *Phys. Rev. Lett.* **91**, 015502 (2003).
- ²⁰J. L. He, E. D. Wu, H. T. Wang, R. P. Liu, and Y. J. Tian, *Phys. Rev. Lett.* **94**, 015504 (2005).
- ²¹M. D. Segall, P. J. D. Lindan, M. J. Probert, C. J. Pickard, P. J. Hasnip, S. J. Clark, and M. C. Payne, *J. Phys.: Condens. Matter* **14**, 2717 (2002).
- ²²D. M. Ceperley and B. J. Alder, *Phys. Rev. Lett.* **45**, 566 (1980).
- ²³J. P. Perdew and A. Zunger, *Phys. Rev. B* **23**, 5048 (1981).
- ²⁴J. S. Lin, A. Qteish, M. C. Payne, and V. Heine, *Phys. Rev. B* **47**, 4174 (1993).
- ²⁵H. J. Monkhorst and J. D. Pack, *Phys. Rev. B* **13**, 5188 (1976).
- ²⁶T. H. Fischer and J. Almlof, *J. Phys. Chem.* **96**, 9768 (1992).
- ²⁷H. Nozaki and S. Itoh, *J. Phys. Chem. Solids* **57**, 41 (1996).
- ²⁸R. Yu, Q. Zhan, and X. F. Zhang, *Appl. Phys. Lett.* **88**, 051913 (2006).
- ²⁹J. C. Crowhurst, A. F. Goncharov, B. Sadigh, C. L. Evans, P. G. Morrall, J. L. Ferreira, and A. J. Nelson, *Science* **311**, 1275 (2006).
- ³⁰Y. Tateyama, T. Ogitsu, K. Kusakabe, S. Tsuneyuki, and S. Itoh, *Phys. Rev. B* **55**, R10161 (1997).
- ³¹X. G. Luo, Z. Y. Liu, X. J. Guo, J. L. He, D. L. Yu, Y. J. Tian, J. Sun, and H. T. Wang, *Chin. Phys. Lett.* **23**, 2175 (2006).
- ³²D. C. Wallace, *Thermodynamics of Crystals* (Wiley, New York, 1972).